Cardiovasc Intervent Radiol (2019) 42:1343–1351
https://doi.org/10.1007/s00270-019-02239-0

LABORATORY INVESTIGATION

Balloon-Expandable Biodegradable Stents Versus Self-Expandable Metallic Stents: A Comparison Study of Stent-Induced Tissue Hyperplasia in the Rat Urethra

Jung-Hoon Park[1,2] · Tae-Hyung Kim[3] · Young Chul Cho[1] · Nader Bakheet[1] · Seung Ok Lee[4] · Seong-Hun Kim[4] · Kun Yung Kim[5]

Received: 26 February 2019 / Accepted: 2 May 2019 / Published online: 13 May 2019

Abstract

Purpose To compare the degrees of stent-induced tissue hyperplasia of balloon-expandable, biodegradable stents (BEBSs) with those of self-expandable metallic stents (SEMSs) in a rat urethral model.

Materials and Methods A total of 20 rats were randomized into two groups. The BEBS group ($n = 10$) received a poly-l-lactic acid (PLLA) biodegradable stent. The SEMS group ($n = 10$) received a nitinol bare stent. All rats were killed eight weeks after stent placement. The degree of stent-induced tissue hyperplasia was assessed by comparing the results of retrograde urethrography and histologic examination between the two groups.

Results Stent placement was technically successful in all rats. Two rats in the BEBS group were excluded due to procedure-related death. The mean luminal diameter of stented urethra on urethrograms was not significantly different at 4 and 8 weeks between the two groups. On histologic analysis, the percentage of granulation tissue area ($p < 0.001$) and the thickness of papillary projection ($p < 0.001$) were significantly higher in the BEBS group compared with the SEMS group. The inflammatory cell infiltration showed a clear tendency to significance ($p = 0.050$). There were no statistical differences in the number of epithelial layers and the thickness of submucosal fibrosis between the two groups.

Conclusion Formation of stent-induced tissue hyperplasia was significantly evident in the rat urethra with similar degrees between the BEBS and the SEMS. The BEBS was associated with a thicker papillary projection and larger granulation tissue area resulting from higher inflammation compared with the SEMS.

Keywords Self-expandable metallic stent · Biodegradable stent · Tissue hyperplasia · Poly-L-lactic acid

Jung-Hoon Park and Tae-Hyung Kim equally contributed to this work as the first authors.

✉ Seong-Hun Kim
shkimgi@jbnu.ac.kr

✉ Kun Yung Kim
kky2kkw@gmail.com

1 Department of Radiology and Research Institute of Radiology, University of Ulsan College of Medicine, 88 Olympic-ro 43-gil, Songpa-gu, Seoul 05505, Republic of Korea

2 Department of Biomedical Engineering Research Center, Asan Medical Center, University of Ulsan College of Medicine, 88 Olympic-ro 43-gil, Songpa-gu, Seoul 05505, Republic of Korea

3 Department of Radiological Science, Kangwon National University, 346 Hwangjo-gil, Dogye-eup, Samcheok-Si, Kangwon-do 25949, Republic of Korea

4 Division of Gastroenterology, Department of Internal Medicine, and Research Institute of Clinical Medicine, Chonbuk National University, 20 Geonji-ro, Deokjin-gu, Jeonju, Chonbuk 54907, Republic of Korea

5 Department of Radiology, and Research Institute of Clinical Medicine of Chonbuk National University-Biomedical Research Institute, Chonbuk National University, 20 Geonji-ro, Deokjin-gu, Jeonju, Chonbuk 54907, Republic of Korea

Introduction

Self-expandable metallic stents (SEMSs) including bare or covered stents have been widely used in the treatment of benign or malignant nonvascular luminal organs with strictures for the past three decades [1–8]. However, stent-induced new stricture formation due to tissue hyperplasia caused by mechanical injury has been a major limitation in stent placement in nonvascular luminal organs such as the urethra, esophagus, and trachea [1, 4, 7]. To overcome this limitation, the placed stents were electively removed at 2–6 months in order to reduce stent-related complications; however, the high recurrence rate after stent removal and stent removal-related complications still remain limitations of this approach [6–8]. Drug-eluting stents have been investigated for suppression of in-stent restenosis caused by tissue hyperplasia after stent placement in various luminal organs [9–12]; however, the current therapeutic strategies remain insufficient in nonvascular luminal organs for a clinical trial.

The SX Ella BD Stent (Ella- CS, Hradec Kralove, Czech Republic) was developed and was commercially available for clinical practice [13]. The BD stent, which was made by polydioxanone, was completely decomposed 11–12 weeks after stent placement and was designed for treatment of benign esophageal strictures and achalasia resistant [13]. An important advantage of biodegradable stents is that no stent removal is indicated due to its biodegradable feature, and thus making it a potentially more cost-effective and patient-friendly treatment option. As biodegradable stents are currently uncovered, granulation tissue can grow through the mesh which can anchor the stent. Even though the extent of tissue hyperplasia induced by biodegradable stents is lower than that of uncovered metallic stents, there is still a high chance of stent obstruction caused by tissue in- and over-growth through the mesh [13–16]. To our knowledge, there has been no study comparing biodegradable stents with SEMS-induced tissue hyperplasia in nonvascular luminal organs. The rat urethral model was used to evaluate the differences between the two stents because it has several advantages including cost-effectiveness, less migration rate, and well established, stent-induced granulation tissue formation [17–19]. Therefore, the purpose of this study was to compare the degrees of stent-induced tissue hyperplasia of balloon-expandable, biodegradable stents (BEBSs) with those of SEMSs in a rat urethral model.

Materials and Methods

Stents Preparation

BEBS was designed and manufactured by Suntech Co., Ltd. (Seoul, Korea) using a poly-L-lactic acid (PLLA) polymer (Mw 200,000). Polymer mini tubes were created in a solution-based dip-coating procedure on metallic male cores. After solvent removal, stent prototypes were manufactured from the polymer mini tubes by laser cutting. Optimization of laser cutting to make the PLLA stents was conducted using a femtosecond laser. The stent was 3 mm in diameter and 8 mm in length with a strut thickness of 120 μm. Four radiopaque markers at both ends of the stent were attached to facilitate precise placement of the stent. After the cutting process, the stent was washed with isopropyl alcohol to remove contamination and it was dried overnight in the air at the room temperature. A PLLA stent was crimped onto a 3-mm diameter and 10-mm length balloon catheter (Genoss, Suwon, Korea) (Fig. 1A).

SEMS was woven from a single thread of 0.10-mm-thick nitinol wire filament into a tubular configuration with six bent points on the upper and lower ends (S&G Biotech, Yongin, Korea). When fully expanded, the bare stent was 3 mm in diameter and 8 mm in length. Two radiopaque markers at both ends of the stent were also attached. The urethral stent introducer set consisted of a 4F Teflon sheath (Cook, Bloomington, IN, USA), including a dilator and a pusher catheter (Fig. 1C).

Animal Study and Stent Placement

This study was approved by the Institutional Animal Care and Use Committee at our institution and conformed to US National Institutes of Health guidelines for humane handling of laboratory animals.

A total of 20, male Sprague–Dawley rats (300–350 g; Orient Bio, Seongnam, Korea) were assigned in two groups, i.e., the BEBS group (n = 10) and the SEMS group (n = 10). The BEBS group received a biodegradable PLLA stent. The SEMS group received a nitinol bare stent. All of the rats were killed 8 weeks after stent placement because granulation tissue formation becomes evident at 8 weeks. All of the rats were supplied with food and water ad libitum and were maintained at a temperature of 24 ± 2 °C with a 12-hour day–night cycle. The body weights of the rats were measured weekly until their kill.

Anesthesia was induced by intramuscular injection of 50 mg/kg zolazepam and tiletamine (Zoletil 50; Virbac, Carros, France) and 10 mg/kg xylazine (Rompun; Bayer HealthCare, Leverkusen, Germany). After disinfection of the external urethral orifice with 0.05% chlorhexidine

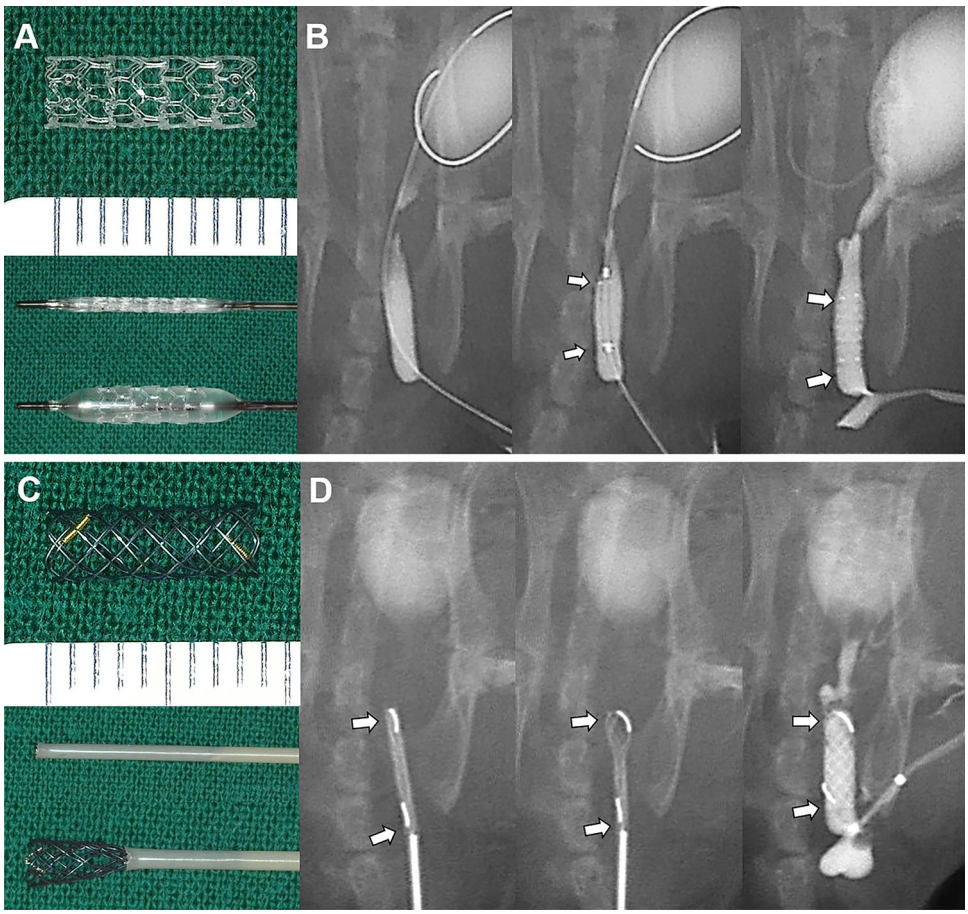

Fig. 1 **A** A balloon-expandable, poly-L-lactic acid biodegradable stent and **C** a self-expandable nitinol stent. Radiographic images show the technical steps of **B** balloon-expandable biodegradable stent (arrows) and **D** self-expandable metallic stent (arrows) placement in a rat urethral model

hydrochloride and lubrication with 2% lidocaine jelly, a retrograde urethrography (RGU) was obtained to determine the position of the bladder neck, urethra, and external urethral sphincter. Using fluoroscopic guidance, a 30-cm and 0.018-in. microguidewire (Transend; Boston Scientific/Medi-Tech, Watertown, MA, USA) was inserted through the urethra and advanced into the urinary bladder. In the BEBS group, a 3 mm in diameter and 10 mm in length balloon catheter (Genoss, Suwon, Korea), which was crimped BEBS, was advanced over the guidewire into the urethra. The balloon catheter was fully inflated to 16 atmospheres as determined by a pressure-gauge monitor and was then deflated simultaneously with the use of contrast medium under continuous fluoroscopic monitoring. The balloon catheter and the guidewire were pulled out of the urethra after stent placement (Fig. 1B). In the SEMS group, a 4F sheath and dilator were passed to the urethra over the microguidewire and advanced until the proximal tip of the dilator reached the upper portion of the urethra. With the sheath left in place, the dilator and the guide wire were removed. A stent in a compressed state was then loaded into the sheath and positioned in the urethra with the use of a pusher catheter under fluoroscopic guidance. The stent was deployed in the urethra by withdrawing the sheath as the pusher catheter was held in place. The sheath and the pusher catheter were pulled out of the urethra after stent deployment (Fig. 1D).

Urethrographic Examination

Fluoroscopically guided (Artis Zee Multipurpose; Siemens, Muenchen, Germany) RGU was performed in right, anterior, oblique projections with the use of a calibrated catheter and with anesthesia in all rats immediately after stent placement in order to verify the position of the stent and passage of contrast medium (Omnipaque 300; GE Healthcare, Cork, Ireland). This procedure was repeated 4 and 8 weeks later to assess changes in diameter within the stent. The luminal diameter was measured on RGUs, and a calibrated catheter, which was constructed in our research laboratory, was used for reference. A software package (Photoshop, version 6.0; Adobe Systems, Palo Alto, CA, USA) was used to acquire digital measurements of the inner luminal diameter of the segment with the stent at three different levels. Measurements were repeated three times at each level, yielding the average value per level, and these values were subsequently averaged to obtain an overall average diameter of the segment of the urethra with

the stent. Analyses of the urethrographic findings were performed on the basis of the consensus of three observers blinded to the study.

Histologic Examination

All of the rats were killed 8 weeks after stent placement by means of administration of inhalable pure carbon dioxide. Surgical exploration of the urethra and urinary bladder were performed. The urethral tissue samples were fixed in 10% neutral buffered formalin for 24 h. Fixed tissue samples were then sectioned transversely at the proximal and distal portions of the segment with the stent. Paraffin blocks were prepared from the tissue samples, and 5-μm-thick sections were obtained with a MR2258 microtome (HostoLine, Pantigliate, Italy). The slides were stained with hematoxylin–eosin (H&E) stains. Histologic evaluation using H&E stain included determining the degree of submucosal inflammatory cell infiltration, the number of epithelial layers, the thickness of submucosal fibrosis, the thickness of papillary projection, and the granulation tissue-related percentage of esophageal cross-sectional area stenosis, calculated as $100 \times (1 - [\text{stenotic stented area}/\text{original stented area}])$. The degree of inflammatory cell infiltration was subjectively determined according to the distribution and density of the inflammatory cells, i.e., graded as 1, mild was given when there was occasional infiltration of single leukocytes visible; 2, mild-to-moderate was given when there was patchy infiltration of leukocytes; 3, moderate was given when there was coalescing leukocytes that individual loci could not be distinguished; 4, moderate-to-severe was given when there was diffuse infiltration of leukocytes throughout the submucosal layer; and 5, severe was given when there was diffuse infiltration with multiple necrotic foci. The average values for the number of epithelial layers, the thickness of submucosal fibrosis, the thickness of papillary projection, and the degree of inflammatory cell infiltration were obtained from averaging eight points around the circumference [18, 19]. Histologic analysis of the urethra was performed with a BX51 microscope (Olympus, Tokyo, Japan). Measurements were obtained by using Image-Pro Plus software (Media Cybernetics, Silver Spring, MD, USA). Analyses of the histologic findings were performed on the basis of the consensus of three observers blinded to the study.

Statistical Analysis

Differences between the groups were analyzed using the Mann–Whitney *U* test, as appropriate. A p value of < 0.05 was considered statistically significant. Statistical analyses were performed using SPSS software (version 23.0; SPSS, IBM, Chicago, IL, USA).

Results

Stent Placement

Stent placement was technically successful in all 20 rats. A small amount of hematuria occurred immediately after stent placement in all rats, but it spontaneously subsided. Two rats in the BEBS group died 3 and 7 days, respectively, after stent placement because of urethral perforation during the procedure. These two rats were excluded from this study. The remaining rats survived until the end of the study without stent-related complications. There were no significant differences in body weights between the BEBS ($n = 8$) and the SEMS ($n = 10$) groups at 4 weeks (451.3 ± 31.2 g vs. 453.2 ± 28.7 g; $p = 0.289$) and 8 weeks (486.3 ± 24.7 g vs. 488.2 ± 25.2 g; $p = 0.311$).

Urethrographic Findings

The urethrographic findings are presented in Table 1, and the examples are shown in Fig. 2. In the 4-week follow-up RGU, there was no significant difference in the luminal diameter of the stented urethra between the two groups (BEBS group; 1.79 ± 0.24 mm vs. SEMS group; 1.86 ± 0.23 mm, $p = 0.210$). These statistical differences were maintained at 8-week follow-up urethrographic results (BEBS group; 1.77 ± 0.27 mm vs. SEMS group; 1.85 ± 0.18 mm, $p = 0.147$). The mean luminal diameter of the stented urethra in the BEBS and the SEMS groups was also not significantly different between 4 and 8 weeks after stent placement. Follow-up RGU showed a severe irregularity around the stent in the BEBS group. In the SEMS group, follow-up RGU showed a straight line filling defect into the stented urethra.

Histologic Findings

The histologic findings are shown in Figs. 3 and 4. The mean percentage of granulation tissue area was significantly higher in the BEBS group compared with SEMS group ($75.8 \pm 8.4\%$ vs. $54.9 \pm 4.4\%$, $p < 0.001$). The mean thickness of papillary projection was also significantly higher in the BEBS group than in the SEMS group (0.69 ± 0.19 mm vs. 0.45 ± 0.15 mm, $p < 0.001$). However, there was no statistically significant difference in the mean number of epithelial layers (4.93 ± 1.23 vs. 4.88 ± 1.45, $p = 0.897$) and the mean thickness of submucosal fibrosis (0.34 ± 0.08 mm vs. 0.37 ± 0.08 mm, $p = 0.183$) between the two groups. The degree of

Table 1 Retrograde urethrographic findings after stent placement in the rat urethra

Location	Luminal diameter of the stented urethra 4 weeks after (mm)		*p* value	Luminal diameter of the stented urethra 8 weeks after (mm)		*p* value
	BEBS group	SMES group		BEBS group	SMES group	
Proximal	1.85 ± 0.23	1.91 ± 0.23	0.585	1.84 ± 0.31	1.89 ± 0.19	0.672
Middle	1.77 ± 0.22	1.83 ± 0.25	0.533	1.74 ± 0.26	1.83 ± 0.20	0.417
Distal	1.74 ± 0.27	1.85 ± 0.20	0.351	1.73 ± 0.26	1.85 ± 0.16	0.234
Total	1.79 ± 0.24	1.86 ± 0.23	0.210	1.77 ± 0.27	1.85 ± 0.18	0.147

Data are the mean ± standard deviation of eight stented urethra in the BEBS group and of 10 stented urethra in the SEMS group

BEBS balloon-expandable biodegradable stent, *SEMS* self-expandable metallic stent

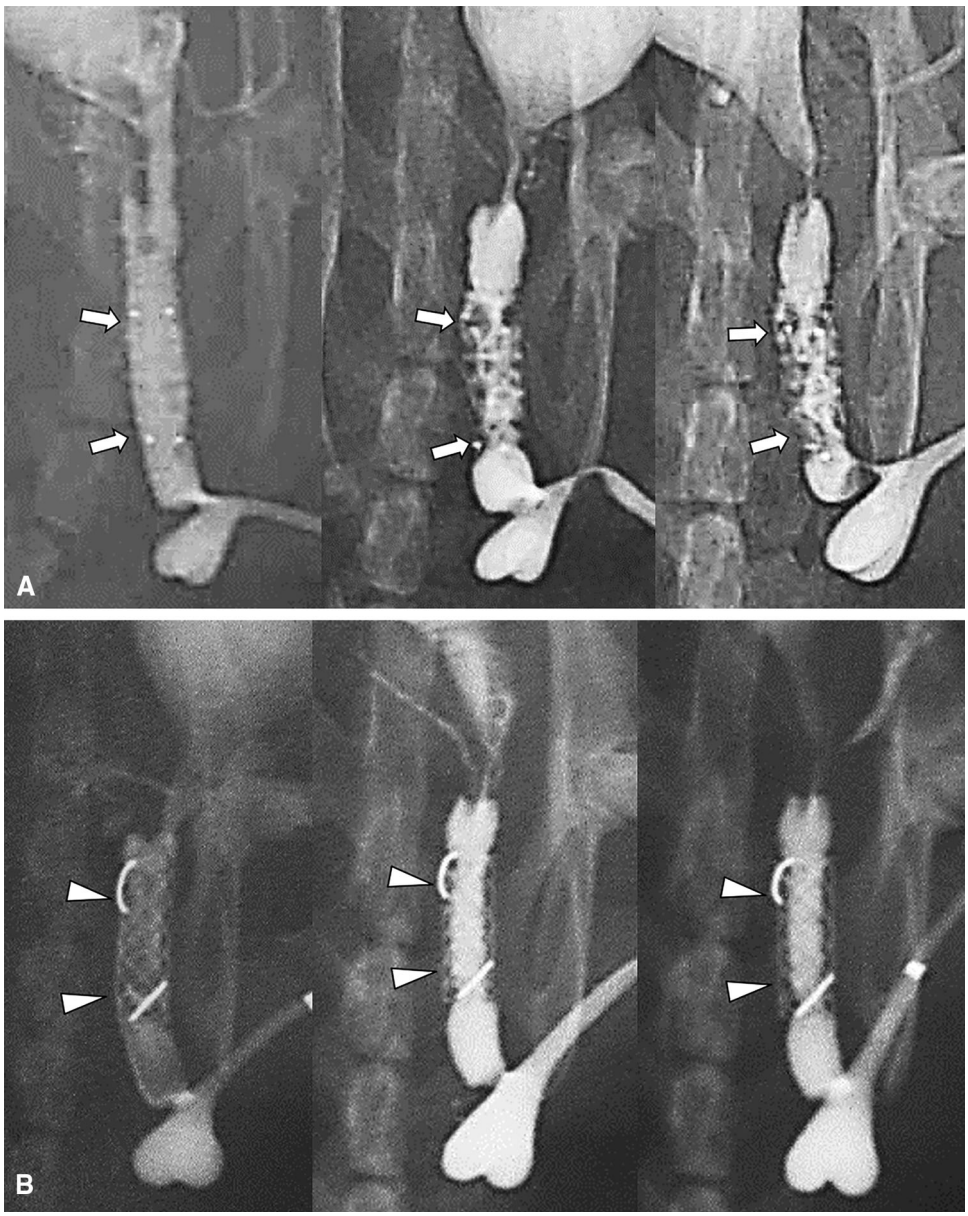

Fig. 2 Retrograde urethrographic (RGU) images obtained immediately, 4 weeks, and 8 weeks after stent placement in the **A** BEBS and **B** SEMS groups. Follow-up RGU shows **A** severe irregularity around the stent (arrows) in the BEBS group and **B** straight line filling defect into the stent (arrowheads) in the SEMS groups caused in each by stent-induced tissue hyperplasia

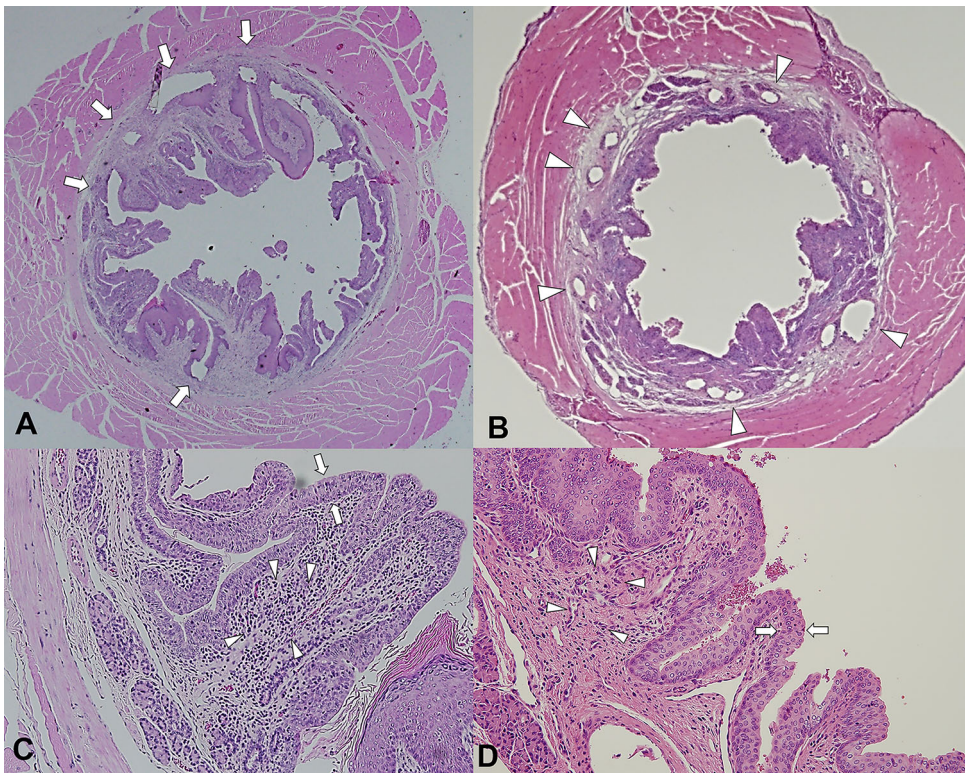

Fig. 3 Representative microscopic images (hematoxylin–eosin staining, magnification ×1.25 **A**, **B**, ×20 **C**, **D**) of histologic sections. All struts removed for the specimens. **A**, **B** Granulation tissue area and thickness of papillary projection were significantly higher in the BEBS group (**A**) compared with the SEMS group (**B**); arrows = biodegradable stent struts and arrowheads = nitinol stent struts. **C**, **D** The density of inflammatory cells (arrowheads) was significantly higher in the BEBS group (**C**) than in the SEMS group (**D**). The number of epithelial layers (arrows) and the thickness of submucosal fibrosis were not significantly different between the two groups

inflammatory cell infiltration showed a clear tendency to significance in the BEBS group compared to that in the SEMS group (3.18 ± 0.83 mm vs. 2.62 ± 0.72 mm, $p = 0.050$).

Discussion

Urethral SEMSs and PLLA biodegradable stent are clinically used for traumatic and recurrent urethral strictures [1, 4, 15, 16]. However, tissue hyperplasia represents a major limitation to long-term stent placement in the urethra [2, 4]. The long-term results of SEMS placement in benign strictures of other nonvascular organs such as the esophagus, tracheobronchial systems, and the lacrimal systems are almost the same as those in the urethra [1, 4, 6, 7]. Biodegradable materials present the advantage of biocompatibility and eliminate the need for stent removal [18]. However, occurrence of granulation tissue formation was reported both PLLA stent for the urethra and polydioxanone stent for the gastrointestinal tract [13–16]. Granulation tissue formation causing restenosis has been the greatest hurdle in the management of benign strictures in nonvascular luminal organs; however, degrees of stent-induced tissue hyperplasia remain unclear between biodegradable stent and metallic stent.

The results of our study demonstrated that the degrees of stent-induced tissue hyperplasia did not differ significantly between BEBS and SEMS groups. Stent-induced tissue hyperplasia in both groups occurred rapidly within 4 weeks after stent placement, and the granulation tissue formation was maintained at 8 weeks without a statistical difference in the luminal diameter of the stented urethra between 4- and 8-week follow-up RGUs. However, histologic examination demonstrated that the thickness of papillary projection and the granulation tissue area in the BEBS group were significantly greater compared to those of the SEMS group, which was well matched with the urethrographic findings.

Balloon-expandable PLLA biodegradable stents have been extensively used for coronary or peripheral artery diseases with a various degree of inflammatory responses in preclinical and clinical studies [20–24]. Permanently implanted PLLA stents into the arteries have been associated with complications such as stent fracture, tissue inflammation, in-stent restenosis, and thrombosis [20, 21]. Those complications might be associated with inflammatory reaction to the PLLA stent. Chen et al. [22] reported that a balloon-expandable PLLA stent caused significant inflammation on endothelial cells induced by PLLA degradation in the porcine coronary artery. The stents made of bioabsorbable polymer is more likely to be associated with an inflammatory reaction compared to a nitinol-based balloon-expandable stent [24]. In our study, PLLA BEBS placement into the rat urethra also significantly increased the inflammatory cell infiltration compared with SEMS

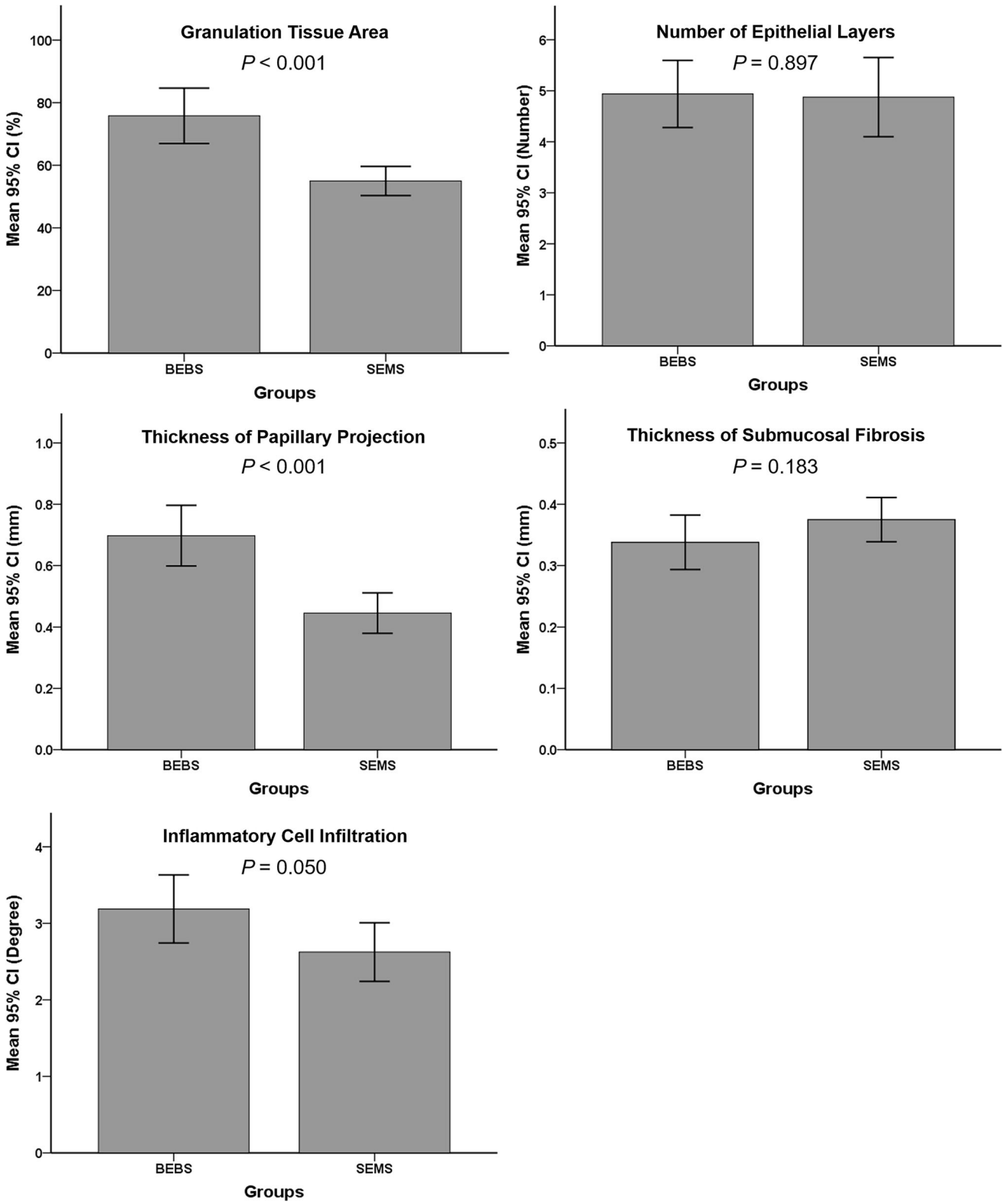

Fig. 4 Histological results of the stented urethra 8 weeks after stent placement in the BEBS and SEMS groups. CI, confidence interval; BEBS, balloon-expandable biodegradable stent; SEMS, self-expandable metallic stent

placement. A PLLA stent may thus induce a relatively higher inflammatory response during its degradation compared with SEMS. Furthermore, a balloon-expandable stent was immediately fully expanded considering the fact that two rats died due to a fully expanded balloon and the stent-induced urethral perforation in the BEBS group. Conversely, SEMS was gradually expanded within 1–3 days after stent placement. Use of a balloon-expandable stent in the BEBS group may be also a significant factor for increasing inflammation, thickness of the papillary projection, and the granulation tissue area.

Wound healing resulting from mechanical injury of a stent on the urethral wall can be divided into at least three, overlapping phases that occur over 4 weeks, i.e., inflammation, proliferation, and remodeling [25–28]. The healing cascade begins immediately following stent-induced mechanical injuries; the proliferative phase then begins between 4 and 14 days and is characterized by increased fibroblasts and myofibroblasts with a decreasing inflammatory phase [27, 28]. In our study, balloon-expandable PLLA stent may prolong or upregulate inflammatory phase during its degradation process. Granulation tissue formation causing restenosis occurs as an excessive proliferative response to mechanical injury after stent placement and has been the significant obstacle for successful stent placement in the management of benign strictures in vascular or nonvascular luminal organs [27–30].

In our study, both BEBS and SEMS placement in the rat urethra was feasible without technical difficulties. Eighteen (90%) of 20 remained alive until their kill without stent-related complications. Stent migration did not occur because of the unique anatomy of the rat urethra and which differs from that in dogs and humans [31]. The stents used in the present study were 3 mm in diameter and 8 mm in length. The size of the stent to be used was decided according to the diameter (2.8 mm) and length (15 mm) of the normal rat urethra weighting approximately 300 g [27]. The rat model is relatively inexpensive and can be easily linked to pathobiological analysis with more and appropriate, available antibodies and transgenic and knockout strains compared with those of large animal models [17–19, 27, 31]. These rat urethral models constitute an efficient approach to stimulate stent-induced tissue hyperplasia as a potential model for reproducing the mechanisms of restenosis as well as our results which can support the necessity of anti-inflammation and/or anti-proliferation drug-eluting stents which can suppress granulation tissue formation after stent placement in nonvascular luminal organs.

Our study has a number of limitations. First, the BEBS and SEMS were placed in the normal rat urethra and the wound healing process after stent placement may differ with benign urethral strictures. Second, the luminal diameter of the stented urethra and quantification of tissue response may differ as a result of the degree of manual injection of contrast medium as well as manual measurement of the values using the program. It was difficult to count inflammatory cells because it was determined subjectively according to the distribution and density of the inflammatory cells. Finally, physical changes including in vitro and in vivo degradation tests in biodegradable stent and histological changes after complete stent degradation were not investigated in current study. Because degradation time of the PLLA stent that used in this study is more than 2 years.

In conclusion, formation of stent-induced tissue hyperplasia was significantly evident in the rat urethra with similar degrees between the BEBS and the SEMS. The BEBS was associated with a thicker papillary projection and larger granulation tissue area resulting from higher inflammation compared with the SEMS. Although BEBS may have therapeutic potential for benign strictures in nonvascular luminal organs with advantage of biocompatibility, stent-induced tissue hyperplasia still remains a significant obstacle for maintaining luminal patency. Drug-eluting biodegradable stents should be investigated to overcome reobstruction caused by stent-induced tissue hyperplasia.

Funding This study was supported by Fund of Biomedical Research Institute (CUH2018-0022), Chonbuk National University Hospital

Compliance with Ethical Standards

Conflict of interest The authors declare that they have no conflict of interest.

Ethical Approval All applicable international, national, and/or institutional guidelines for the care and use of animals were followed.

Informed Consent For this type of study, informed consent is not required.

References

1. Song HY, Cho KS, Sung KB, Han YM, Kim YG, Kim CS. Self-expandable metallic stents in high-risk patients with benign prostatic hyperplasia: long-term follow-up. Radiology. 1995;195:655–60.
2. Song HY, Lee DH, Seo TS, et al. Retrievable covered nitinol stents: experiences in 108 patients with malignant esophageal strictures. J Vasc Interv Radiol. 2002;13:285–93.
3. Park JH, Lee JH, Song HY, et al. Over-the-wire versus through-the-scope stents for the palliation of malignant gastric outlet obstruction: a retrospective comparison study. Eur Radiol. 2016;26:4249–58.
4. Song HY, Park H, Suh TS, et al. Recurrent traumatic urethral strictures near the external sphincter: treatment with a covered, retrievable, expandable nitinol stent—initial results. Radiology. 2003;226:433–40.

5. Park JH, Song HY, Kim JH, et al. Polytetrafluoroethylene-covered retrievable expandable nitinol stents for malignant esophageal obstructions: factors influencing the outcome of 270 patients. AJR Am J Roentgenol. 2012;199:1380–6.
6. Kim JH, Shin JH, Song HY, Shim TS, Yoon CJ, Ko GY. Benign tracheobronchial strictures: long-term results and factors affecting airway patency after temporary stent placement. AJR Am J Roentgenol. 2007;188:1033–8.
7. Kim JH, Song HY, Choi EK, Kim KR, Shin JH, Lim JO. Temporary metallic stent placement in the treatment of refractory benign esophageal strictures: results and factors associated with outcome in 55 patients. Eur Radiol. 2009;19:384–90.
8. Park JH, Song HY, Park JY, et al. Temporary stent placement with concurrent chemoradiation therapy in patients with unresectable oesophageal carcinoma: Is there an optimal time for stent removal? Eur Radiol. 2013;23:1940–5.
9. Shaikh M, Kichenadasse G, Choudhury NR, Butler R, Garg S. Non-vascular drug eluting stents as localized controlled drug delivery platform: preclinical and clinical experience. J Control Release. 2013;172:105–17.
10. Han K, Park JH, Yang SG, et al. EW-7197 eluting nano-fiber covered self-expandable metallic stent to prevent granulation tissue formation in a canine urethral model. PLoS ONE. 2018;13:e0192430.
11. Kim EY, Song HY, Kim JH, et al. IN-1233 eluting covered metallic stent to prevent hyperplasia: experimental study in a rabbit esophageal model. Radiology. 2013;267:396–404.
12. Lee SS, Shin JH, Han JM, et al. Histologic influence of paclitaxel-eluting covered metallic stents in a canine biliary model. Gastrointest Endosc. 2009;69:1140–7.
13. Sigounas DE, Siddhi S, Plevris JN. Biodegradable esophageal stents in benign and malignant strictures: a single center experience. Endosc Int Open. 2016;4:618–23.
14. Griffiths EA, Gregory CJ, Pursnani KG, Ward JB, Stockwell RC. The use of biodegradable (SX-ELLA) oesophageal stents to treat dysphagia due to benign and malignant oesophageal disease. Surg Endosc. 2012;26:2367–75.
15. Isotalo T, Talja M, Valimaa T, Tormala P, Tammela TL. A bioabsorbable selfexpandable, self-reinforced poly-L-lactic acid urethral stent for recurrent urethral strictures: long-term results. J Endourol. 2002;16:759–62.
16. Isotalo T, Tammela TL, Talja M, Valimaa T, Tormala P. A bioabsorbable self-expandable, self-reinforced poly-L-lactic acid urethral stent for recurrent urethral strictures: a preliminary report. J Urol. 1998;160:2033–6.
17. Li YD, Song HY, Kim JH, et al. Evaluation of formation of granulation tissue caused by metallic stent placement in a rat urethral model. J Vasc Interv Radiol. 2010;21:1884–90.
18. Kim KY, Park JH, Kim DH, et al. Sirolimus-eluting biodegradable poly-L-lactic acid stent to suppress granulation tissue formation in the rat urethra. Radiology. 2018;286:140–8.
19. Park JH, Kim JH, Kim EY, et al. Bioreducible polymer-delivered siRNA targeting MMP-9: suppression of granulation tissue formation after bare metallic stent placement in a rat urethral model. Radiology. 2014;271:87–95.
20. Nishio S, Kosuga K, Igaki K, et al. Long-term (> 10 years) clinical outcomes of first-in-human biodegradable poly-L-lactic acid coronary stents: Igaki-Tamai stents. Circulation. 2012;125:2343–53.
21. Waksman R. Update on bioabsorbable stents: from bench to clinical. J Interv Cardiol. 2006;19:414–21.
22. Cehn D, Su Z, Weng L, et al. Effect of inflammation on endothelial cells induced by poly-L-lactic acid degradation in vitro and in vivo. J Biomater Sci Polym Ed. 2018;29:1909–19.
23. Bünger CM, Grabow N, Sternberg K, et al. A biodegradable stent based on poly(L-lactide) and poly(4-hydroxybutyrate) for peripheral vascular application: preliminary experience in the pig. J Endovasc Ther. 2007;14:725–33.
24. Lee JH, Kim SJ, Park SI, et al. Development of a new hybrid biodegradable drug-eluting stent for the treatment of peripheral artery disease. Biomed Res Int. 2016;2016:6915789.
25. Li J, Chen J, Kirsner R. Pathophysiology of acute wound healing. Clin Dermatol. 2007;5:9–18.
26. Diegelmann RF, Evans MC. Wound healing: an overview of acute, fibrotic and delayed healing. Front Biosci. 2004;9:283–9.
27. Kim JH, Song HY, Park JH, et al. IN-1233, an ALK-5 inhibitor: prevention of granulation tissue formation after bare metallic stent placement in a rat urethral model. Radiology. 2010;255:75–82.
28. Park JH, Park W, Cho S, et al. Nanofunctionalized stent-mediated local heat treatment for the suppression of stent-induced tissue hyperplasia. ACS Appl Mater Interfaces. 2018;10:29357–66.
29. Teirstein PS, Massullo V, Jani S, et al. Catheter-based radiotherapy to inhibit restenosis after coronary stenting. N Engl J Med. 1997;336:1697–703.
30. Shin JH, Song HY, Choi CG, et al. Tissue hyperplasia: influence of a paclitaxel eluting covered stent—preliminary study in a canine urethral model. Radiology. 2005;234:438–44.
31. Kim EY, Shin JH, Jung YY, Shin DH, Song HY. A rat esophageal model to investigate stent-induced tissue hyperplasia. J Vasc Interv Radiol. 2010;21:1287–91.